

Technical University of Denmark



## Crystallographic dependence of the lateral undercut wet etch rate of Al<sub>0.5</sub>In<sub>0.5</sub>P in diluted HCl for III-V sacrificial release

**Ansbæk, Thor; Semenova, Elizaveta; Yvind, Kresten; Hansen, Ole**

*Published in:*

Journal of Vacuum Science and Technology. Part B. Microelectronics and Nanometer Structures

*Link to article, DOI:*

[10.1116/1.4771971](https://doi.org/10.1116/1.4771971)

*Publication date:*

2013

*Document Version*

Publisher's PDF, also known as Version of record

[Link back to DTU Orbit](#)

*Citation (APA):*

Ansbæk, T., Semenova, E., Yvind, K., & Hansen, O. (2013). Crystallographic dependence of the lateral undercut wet etch rate of Al<sub>0.5</sub>In<sub>0.5</sub>P in diluted HCl for III-V sacrificial release. *Journal of Vacuum Science and Technology. Part B. Microelectronics and Nanometer Structures*, 31(1), 011209. DOI: 10.1116/1.4771971

## DTU Library

Technical Information Center of Denmark

---

### General rights

Copyright and moral rights for the publications made accessible in the public portal are retained by the authors and/or other copyright owners and it is a condition of accessing publications that users recognise and abide by the legal requirements associated with these rights.

- Users may download and print one copy of any publication from the public portal for the purpose of private study or research.
- You may not further distribute the material or use it for any profit-making activity or commercial gain
- You may freely distribute the URL identifying the publication in the public portal

If you believe that this document breaches copyright please contact us providing details, and we will remove access to the work immediately and investigate your claim.

## Crystallographic dependence of the lateral undercut wet etch rate of Al<sub>0.5</sub>In<sub>0.5</sub>P in diluted HCl for III–V sacrificial release

Thor Ansbæk, Elizaveta S. Semenova, Kresten Yvind, and Ole Hansen

Citation: *J. Vac. Sci. Technol. B* **31**, 011209 (2013); doi: 10.1116/1.4771971

View online: <http://dx.doi.org/10.1116/1.4771971>

View Table of Contents: <http://avspublications.org/resource/1/JVTBD9/v31/i1>

Published by the AVS: Science & Technology of Materials, Interfaces, and Processing

### Related Articles

Nanometer scale high-aspect-ratio trench etching at controllable angles using ballistic reactive ion etching  
*J. Vac. Sci. Technol. B* **31**, 010604 (2013)

Plasma-assisted cleaning by metastable-atom neutralization  
*J. Vac. Sci. Technol. B* **31**, 011603 (2013)

Fabrication of indium tin oxide bump/pit structures on GaN-based light emitting diodes  
*J. Vac. Sci. Technol. B* **31**, 011804 (2013)

Kinetics of the deposition step in time multiplexed deep silicon etches  
*J. Vac. Sci. Technol. B* **31**, 011208 (2013)

Large-area fabrication of high aspect ratio tantalum photonic crystals for high-temperature selective emitters  
*J. Vac. Sci. Technol. B* **31**, 011802 (2013)

### Additional information on *J. Vac. Sci. Technol. B*

Journal Homepage: <http://avspublications.org/jvstb>

Journal Information: [http://avspublications.org/jvstb/about/about\\_the\\_journal](http://avspublications.org/jvstb/about/about_the_journal)


Top downloads: [http://avspublications.org/jvstb/top\\_20\\_most\\_downloaded](http://avspublications.org/jvstb/top_20_most_downloaded)

Information for Authors: [http://avspublications.org/jvstb/authors/information\\_for\\_contributors](http://avspublications.org/jvstb/authors/information_for_contributors)

## ADVERTISEMENT

# Instruments for advanced science

**Gas Analysis**



- dynamic measurement of reaction gas streams
- catalysis and thermal analysis
- molecular beam studies
- dissolved species probes
- fermentation, environmental and ecological studies

**Surface Science**



- UHV TPD
- SIMS
- end point detection in ion beam etch
- elemental imaging - surface mapping

**Plasma Diagnostics**



- plasma source characterization
- etch and deposition process reaction kinetic studies
- analysis of neutral and radical species

**Vacuum Analysis**



- partial pressure measurement and control of process gases
- reactive sputter process control
- vacuum diagnostics
- vacuum coating process monitoring

contact Hiden Analytical for further details

**HIDEN ANALYTICAL**

[info@hideninc.com](mailto:info@hideninc.com)  
[www.HidenAnalytical.com](http://www.HidenAnalytical.com)

CLICK to view our product catalogue 

# Crystallographic dependence of the lateral undercut wet etch rate of $\text{Al}_{0.5}\text{In}_{0.5}\text{P}$ in diluted HCl for III–V sacrificial release

Thor Ansbæk, Elizaveta S. Semenova, and Kresten Yvind<sup>a)</sup>

Department of Photonics Engineering, Technical University of Denmark, Ørsteds Plads, 2800 Kgs. Lyngby, Denmark

Ole Hansen

Department of Micro- and Nanotechnology, Technical University of Denmark, Ørsteds Plads, Building 345E, 2800 Kgs. Lyngby, Denmark and CINF—Center for Individual Nanoparticle Functionality, Technical University of Denmark, Building 345E, 2800 Kgs. Lyngby, Denmark

(Received 7 June 2012; accepted 29 November 2012; published 19 December 2012)

The authors investigated the use of InAlP as a sacrificial layer lattice-matched to GaAs when diluted hydrochloric acid is used for sacrificial etching. They show that InAlP can be used to fabricate submicrometer air gaps in micro-opto-electro-mechanical systems and that a selectivity toward GaAs larger than 500 is achieved. This selectivity enables fabrication control of the nanometer-size structures required in photonic crystal and high-index contrast subwavelength grating structures. The crystallographic dependence of the lateral etch rate in InAlP is shown to be symmetric around the  $\langle 110 \rangle$  directions where an etch rate of  $0.5 \mu\text{m}/\text{min}$  is obtained at  $22^\circ\text{C}$  in  $\text{HCl} : 2\text{H}_2\text{O}$ . Since the etch rate in the  $\langle 100 \rangle$  directions exceeds by ten times that of the  $\langle 110 \rangle$  directions, InAlP may be used in sacrificial release of high-aspect ratio structures. Free-hanging structures with length to air-gap aspect ratios above 600 are demonstrated by use of critical point drying following the sacrificial etch. © 2013 American Vacuum Society.

[<http://dx.doi.org/10.1116/1.4771971>]

## I. INTRODUCTION

Sacrificial wet etching of compound semiconductors is a necessary step during fabrication of nanophotonics devices such as photonic crystals, tunable vertical-cavity surface-emitting lasers, and photodetectors.<sup>1–4</sup> By removal of sacrificial material, an air-gap may be fabricated and, thus, high-index contrast and movable mechanical structures are enabled. Preferably, the sacrificial wet etch should be isotropic, selective to other materials present, and have an etch rate on the order of  $1 \mu\text{m}/\text{min}$ . For crystalline materials, however, the etch process is usually anisotropic, though the two other requirements may be met. The etch selectivity must be high since during fabrication of nanophotonic devices, the wet etch must remove one material without significantly affecting nanometer-sized patterns realized in other materials.

The device topology often requires that multiple binary, ternary, and/or quaternary materials are present at the same time, and thus it becomes a challenging task to find an appropriate etch chemistry. Compared to silicon microelectromechanical systems where hydrofluoric acid is well-established for sacrificial etching of silicon oxide and a significantly smaller variety of materials are present, sacrificial etching of III–V compound semiconductor materials is much more complicated. For a comprehensive review on III–V sacrificial etching, we refer to the article of Hjort.<sup>5</sup> For devices based on GaAs substrates, the main sacrificial materials reported in literature are  $\text{Al}_x\text{Ga}_{1-x}\text{As}$ ,  $\text{Al}_{0.5}\text{In}_{0.5}\text{P}$  and  $\text{In}_{0.5}\text{Ga}_{0.5}\text{P}$ , since they may all be grown lattice-matched to GaAs substrates.<sup>6–8</sup>

Anhydrous (water-free) citric acid ( $\text{C}_6\text{H}_8\text{O}_7$ ) mixed with hydrogen peroxide ( $\text{H}_2\text{O}_2$ ) and ammonium hydroxide ( $\text{NH}_4\text{OH}$ ) has been reported for etching GaAs selective to  $\text{Al}_{0.15}\text{Ga}_{0.85}\text{As}$  with selectivities up to 100.<sup>9</sup> Hydrofluoric acid is favored for etching  $\text{Al}_x\text{Ga}_{1-x}\text{As}$  with  $x \geq 0.5$  where high etch rates and selectivities are obtained simultaneously.<sup>7,10</sup>  $\text{Al}_x\text{Ga}_{1-x}\text{As}$  can be difficult to use as a sacrificial material since it may also appear both in the fabrication of high-reflectivity distributed Bragg reflectors and piezoelectric layers and, hence, high selectivity toward  $\text{Al}_x\text{Ga}_{1-x}\text{As}$  is often desired. In order to selectively undercut GaAs, sacrificial layers of AlInP or InGaP have been reported, with hydrochloric acid (HCl) used for sacrificial wet etching.<sup>6,11</sup> The lateral etch rate of InGaP has been reported for different crystallographic orientations but not for AlInP. Studies on AlInP have focused only on the etch rate of the (100) plane.<sup>8</sup>

Here, we report the first results on the lateral wet etch rate of AlInP using an  $\text{HCl} : x\text{H}_2\text{O}$  etch solution. We show that AlInP can be etched at a rate of  $0.5 \mu\text{m}/\text{min}$  with a selectivity toward GaAs exceeding 500. Furthermore, we show that released mechanical structures can be achieved by use of critical point drying to overcome stiction. This is of critical importance for successful release of large structures where the mechanical stiffness may be insufficient to overcome the capillary forces occurring during drying, due to the surface tension of the liquid.

## II. EXPERIMENTAL METHODS

For epitaxial growth, 2 in. (100) GaAs wafers with the major flat cut along  $[0\bar{1}1]$  were used. Epitaxial growth was conducted in an Emcore D-125 Turbodisc®-equipped metal-organic vapor phase epitaxy rotating disk reactor. The

<sup>a)</sup>Electronic mail: ky@fotonik.dtu.dk

sacrificial  $\text{Al}_{0.53}\text{In}_{0.47}\text{P}$  layer was grown at  $610^\circ\text{C}$  to a thickness of  $540\text{ nm}$  and capped with a  $280\text{ nm}$  thick GaAs layer. The lattice mismatch,  $\Delta a/a_{\text{GaAs}}$ , was characterized by x-ray diffraction to be less than  $10^{-3}$ . The wafers were patterned using photoresist (AZ5214E) and conventional UV lithography. A pattern of  $40\text{-}\mu\text{m}$ -squares rotated at angles from  $0^\circ$  to  $45^\circ$  in steps of  $2.65^\circ$  was then transferred to GaAs by  $\text{Cl}_2/\text{Ar}$  inductively coupled plasma etching at  $20^\circ\text{C}$ . During over-etching, the exposed AlInP was dry-etched at a lower etch rate. The samples were then etched with one part hydrochloric acid diluted in  $x$  parts of deionized water ( $37\%$   $\text{HCl} : x\text{H}_2\text{O}$ ) at room temperature. After etching, the samples were rinsed in deionized water and dried. Samples for lateral etch rate measurements were dried in  $\text{N}_2$ , while samples with released beams were rinsed in 2-isopropanol and dried using critical point drying. Since the etch process is surface reaction limited, the rate is strongly temperature-dependent<sup>6</sup> and, therefore, the temperature was monitored using a thermometer to ensure reproducible results. The undercut was imaged using an optical microscope fitted with a Nomarski prism for differential interference contrast (DIC), while the etch profile was imaged using scanning electron microscopy (SEM).

### III. RESULTS AND DISCUSSION

We find that wet etching of AlInP in  $\text{HCl} : 2\text{H}_2\text{O}$  is limited by  $\{111\}\text{A}$  planes that etch at  $0.5\text{ }\mu\text{m}/\text{min}$  at  $22^\circ\text{C}$ . Figure 1 shows the etch profiles of AlInP in (a) the  $[0\bar{1}\bar{1}]$  and

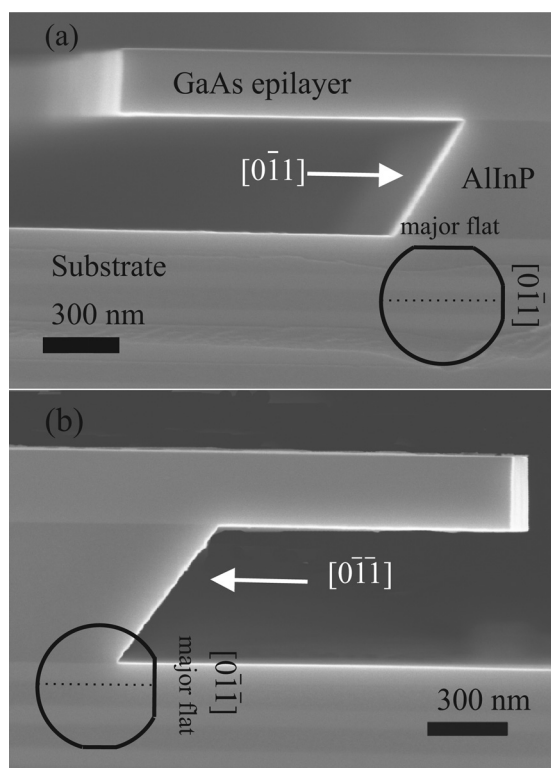


Fig. 1. Scanning electron microscope image of the etch-profile along (a) minor flat  $[0\bar{1}\bar{1}]$  and (b) major flat  $[0\bar{1}\bar{1}]$ . The sample has been cleaved using a diamond-scribe.

(b) the  $[0\bar{1}\bar{1}]$  directions after etching in  $\text{HCl} : 2\text{H}_2\text{O}$ . Similar results have been shown for the  $[0\bar{1}\bar{1}]$  direction by Lee *et al.*<sup>11</sup> The etch profile in Fig. 1(a) is typical of anisotropic reaction-limited etching with a slope of  $54.7^\circ$  corresponding to the angle between the  $(1\bar{1}\bar{1})$  plane and the  $(100)$  surface. The angle in Fig. 1(b) is around  $125^\circ$ , which shows that the column-III-terminated  $\{111\}\text{A}$  plane is the slowest etching plane.<sup>5</sup>

The DIC images in Fig. 2 show the undercut (light grey) of unmasked squares (dark grey) aligned to (a) the  $[0\bar{1}\bar{1}]$ , (b)  $23.8^\circ$  from the  $[0\bar{1}\bar{1}]$ , and (c) the  $[0\bar{1}0]$  direction, respectively. The etched pattern is limited by the low etch rate of the  $\{111\}\text{A}$  planes, which intersects the  $(100)$  plane along  $\langle 110 \rangle$  directions and thus the outline of the etched pattern will proceed until it is bounded by  $\langle 110 \rangle$  directions.

Figure 3 shows the crystallographic orientation dependence of the etch rate in AlInP as a function of the angle relative to the  $[0\bar{1}\bar{1}]$  direction for two  $\text{HCl}$ -based etch solutions. The etch rate in the  $\langle 100 \rangle$  directions is several times higher than that in the  $\langle 110 \rangle$  directions, and this anisotropy is seen to be dependent on the  $\text{HCl}$  concentration, whereas the etch rate in the  $[0\bar{1}\bar{1}]$ -direction is (within experimental error) the same in the two etch solutions while the etch rate in the  $[0\bar{1}0]$ -direction increases with increasing  $\text{HCl}$  concentration. Figure 3 shows that the etch rate is symmetric around the  $[0\bar{1}0]$  direction but slightly skewed toward the  $[0\bar{1}\bar{1}]$  direction, which is clearly seen in Fig. 2(b). Similar results have been observed during wet etching of InGaP in  $\text{HCl}$  and attributed to atomic surface reconstruction during etching.<sup>8</sup> The lithographic pattern was aligned to the wafer major flat, specified to within  $3^\circ$  of the  $[0\bar{1}\bar{1}]$ -direction, and the resulting possible misalignment to the crystal direction may explain the off-set of the symmetry point of the curve from the  $[0\bar{1}0]$ -direction.

Previous studies have shown that wet etching of AlInP in  $\text{HCl} : \text{H}_2\text{O}$  has perfect selectivity (above  $10^6$ ) to GaAs.<sup>5,6</sup> In contrast to this, we find a GaAs etch rate on the order of  $1\text{ nm}/\text{min}$  in the  $\langle 110 \rangle$  directions; that is, the selectivity of GaAs to AlInP is  $>1:500$ . The etch rate was deduced from line width measurements on lines of nominal  $130\text{ nm}$  width and  $460\text{ nm}$  pitch. Line widths were measured using SEM before and after  $10\text{ min}$  of wet etching in  $\text{HCl} : 2\text{H}_2\text{O}$ . Etching of GaAs is usually mediated by an oxidizing agent and, thus, the nonzero etch rate is an unexpected result. It is commonly assumed that  $\text{HCl}$  does not etch GaAs and, in general, the oxidizing agent  $\text{H}_2\text{O}_2$  is added for GaAs wet etching. Four different possible explanations for the incomplete selectivity are identified: anodic etching due to the presence of metal pads, photochemical etching, crystal quality, and oxidation by  $\text{H}_2\text{O}$ . However, we do not see any sign of surface pitting, which is commonly seen in anodic etching.<sup>12</sup> Photochemical wet etching of GaAs has also been reported but at higher light intensities.<sup>13</sup> Since the etch rate was measured on GaAs grown on top of AlInP, an increased etch rate of the GaAs epilayer could be due to a higher number of crystal defects or impurities, such as the presence of Al, In, or P. Also,  $\text{H}_2\text{O}$  can act as an oxidizing agent in acidic solutions where  $\text{Ga}_2\text{O}_3$  is formed, and although the oxidation



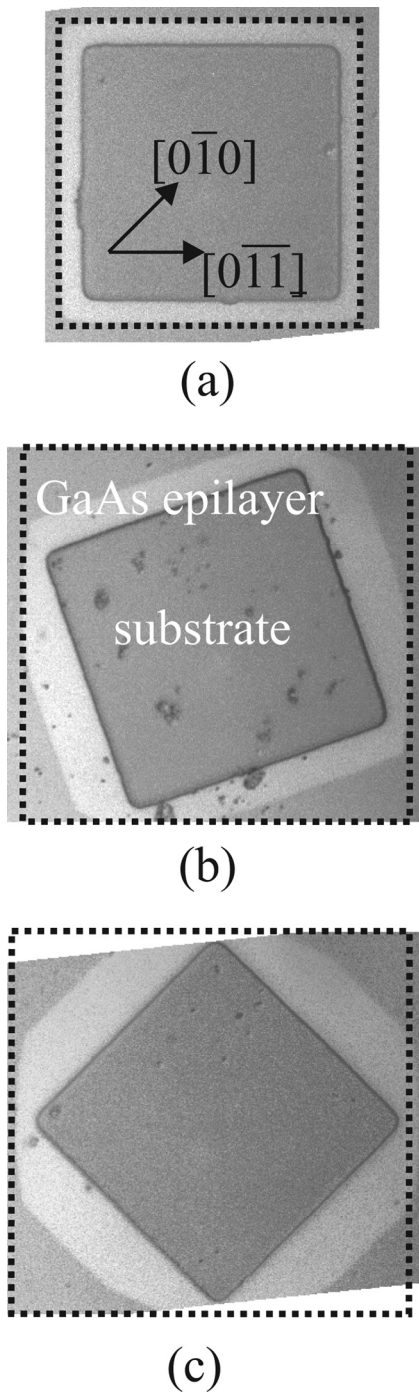


FIG. 2. Optical microscope image showing structures etched out of  $40 \times 40 \mu\text{m}^2$  square mask windows aligned to (a) the  $[0\bar{1}\bar{1}]$  direction, (b)  $23.8^\circ$  from the  $[0\bar{1}\bar{1}]$  direction, and (c) the  $[0\bar{1}0]$  direction. The undercut region is the bright area. The samples were etched for 15 min in  $\text{HCl} : 5\text{H}_2\text{O}$ . The limiting  $\langle 110 \rangle$  directions are outlined with a dashed line.

rate is very low ( $\approx 0.5 \text{ nm/h}$  for pure  $\text{H}_2\text{O}$ ), it can significantly increase when the  $\text{pH}$ -value of the mixture is lowered.<sup>14</sup> Further studies are needed to clarify the unexpected etching of GaAs.

Undercutting of support structures is an issue in mechanical systems. The anisotropy of the wet etch can be exploited to reduce undercutting of the supports relative to structures that are to be fully released and thus fully

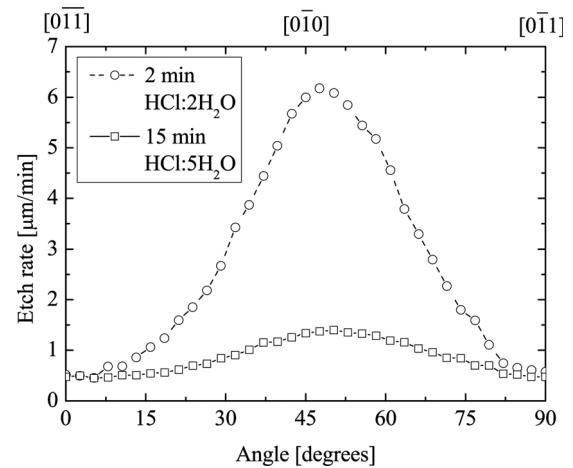


FIG. 3. Plot of the etch rate of  $\text{Al}_{0.5}\text{In}_{0.5}\text{P}$  in different directions relative to the  $\langle 110 \rangle$  direction. The etch rate is highest in the  $\langle 100 \rangle$  direction.

undercut. This is achieved by aligning the support structures to the  $\langle 110 \rangle$  directions, while the free-hanging structures are aligned to the  $\langle 100 \rangle$  directions. Another critical issue is stiction, which is related to the surface tension and wetting properties of the liquids used and the stiffness of the structures to be released. Stiction is a well-known problem and may be avoided by critical point drying.<sup>15</sup> In this technique, the rinse liquid is substituted with liquid  $\text{CO}_2$ , which is brought to its critical point. By maintaining the temperature above the critical point, the pressure is then lowered in the gas-phase. Figure 4 shows released cantilevers with an air-gap spacing of  $0.5 \mu\text{m}$ . The longest cantilevers are  $350 \mu\text{m}$  long and the cantilevers to the left are  $40 \mu\text{m}$  wide, while the cantilevers to the right are  $10 \mu\text{m}$  wide. All cantilevers have been successfully released, i.e., none of them are stuck to the substrate surface. The inset in Fig. 4 shows a magnification of a shorter cantilever, where the shadow due to the air-gap is clearly visible. The slight curvature of the cantilevers that is observed in Fig. 4 may be explained by a thin residue layer left over from incomplete etching. Note in Fig. 1 that no etch product residual is observable.

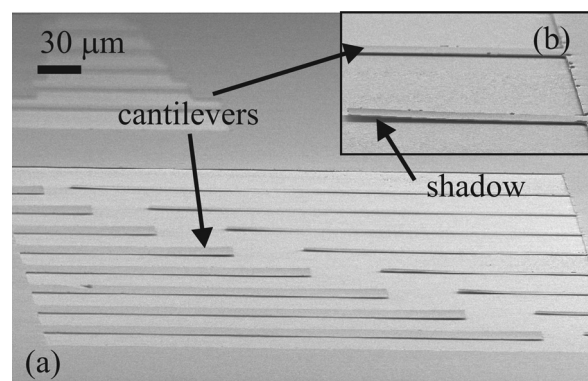


FIG. 4. Scanning electron microscope image of suspended beams released by critical point drying. The image (a) shows an overview of 10 and  $40 \mu\text{m}$  wide beams. The inset (b) shows a zoom-in on a single cantilever.

#### IV. SUMMARY AND CONCLUSION

The lateral etch rate of AlInP in diluted hydrochloric acid and its use as a sacrificial layer have been investigated. We find that the etching of AlInP in diluted hydrochloric acid shows a selectivity toward GaAs of 1:500. This compares favorably with the highest selectivity reported for InGaP of 1:100 using the same etchant. Furthermore, the etch rate of AlInP in HCl is much higher than that of InGaP. The more rapid sacrificial release makes high-aspect ratio structures more feasible. Therefore, AlInP is a good candidate for sacrificial layers in micro-opto-electro-mechanical systems.

#### ACKNOWLEDGMENTS

The authors would like to thank Jong Min Kim for his role in AlInP growth. The Center for Individual Nanoparticle Functionality (CINF) is sponsored by The Danish National Research Foundation.

<sup>1</sup>M. Schubert, T. Suhr, S. Ek, E. S. Semenova, J. M. Hvam, and K. Yvind, *Appl. Phys. Lett.* **97**, 191109 (2010).

<sup>2</sup>K. Hennessy *et al.*, *Nature* **445**, 896 (2007).

<sup>3</sup>M. C. Y. Huang, Y. Zhou, and C. J. Chang-Hasnain, *Nature Photon.* **2**, 180 (2008).

<sup>4</sup>W. Jie, H. Qin, Y. Xiao-Hong, W. Xiu-Ping, N. Hai-Qiao, and H. Ji-Fang, *J. Vac. Sci. Technol. B* **29**, 041208 (2011).

<sup>5</sup>K. Hjort, *J. Micromech. Microeng.* **6**, 370 (1996).

<sup>6</sup>J. R. Lothian, J. M. Kuo, W. S. Hobson, E. Lane, F. Ren, and S. J. Pearton, *J. Vac. Sci. Technol. B* **10**, 1061 (1992).

<sup>7</sup>E. Yablonovitch, T. Gmitter, J. P. Harbison, and R. Bhat, *Appl. Phys. Lett.* **51**, 2222 (1987).

<sup>8</sup>M. J. Cich, J. A. Johnson, G. M. Peake, and O. B. Spahn, *Appl. Phys. Lett.* **82**, 651 (2003).

<sup>9</sup>T. Kitano, S. Izumi, H. Minami, T. Ishikawa, K. Sato, T. Sonoda, and M. Otsubo, *J. Vac. Sci. Technol. B* **15**, 167 (1997).

<sup>10</sup>P. Kumar, S. Kanakaraju, and D. L. DeVoe, *Appl. Phys. A* **88**, 711 (2007).

<sup>11</sup>J. W. Lee, S. J. Pearton, C. R. Abernathy, W. S. Hobson, F. Ren, and C. S. Wu, *J. Electrochem. Soc.* **142**, L100 (1995).

<sup>12</sup>C. M. Finnie, X. Li, and P. W. Bohn, *J. Appl. Phys.* **86**, 4997 (1999).

<sup>13</sup>D. V. Podlesnik, H. H. Gilgen, and R. M. Osgood, *Appl. Phys. Lett.* **45**, 563 (1984).

<sup>14</sup>H.-H. Wang, C.-J. Huang, Y.-H. Wang, and M.-P. Houg, *Jpn. J. Appl. Phys., Part 2* **37**, L67 (1998).

<sup>15</sup>T. F. Anderson, *J. Appl. Phys.* **21**, 724 (1950).